

Study and Analysis of Insect and Bird Flight Mechanism: Design, Analysis and Development of Micro Air Vehicle

A MAJOR PROJECT REPORT

Submitted by

GOVIND SINGH DHAMI (R180206021)

SMITI MAINI (R180206055)

8th Semester

Under the guidance of

Dr. Om Prakash

Dr. Parag Mantri

In partial fulfillment for the award of the degree

of

BACHELOR OF TECHNOLOGY

IN

AEROSPACE ENGINEERING



COLLEGE OF ENGINEERING STUDIES

UNIVERSITY OF PETROLEUM AND ENERGY STUDIES

DEHRADUN- 248 006

May 2010



UPES - Library



D11071

DHA-2010RT



UNIVERSITY OF PETROLEUM & ENERGY STUDIES

(ISO 9001:2000 Certified)

CERTIFICATE

This is to certify that the Major Project report titled “**Study and Analysis of Insect and Bird Flight Mechanism: Design, Analysis and Development of Micro Air Vehicle**” submitted to University of Petroleum & Energy Studies by **GOVIND SINGH DHAMI (R180206021) and SMITI MAINI (R180206055)** in partial fulfillment of degree of Bachelor of Technology in Aerospace Engineering, is a bonafide record of the work carried out by them under our supervision and guidance.

Date: 09-05-2010

Place: DEHRADUN

(Dr. Om Prakash)

Head of Department,
Aerospace Department
UPES

(Dr. Parag Mantri)

Assistant Professor,
Aerospace Department
UPES

ACKNOWLEDGEMENT

We feel greatly privileged to express our sincere gratitude to our mentor Dr. Om Prakash, HOD Aerospace Deptt., for his timely guidance, valuable suggestions and enthusiastic support towards us, in the completion of this project work.

We profusely thank Dr. Parag Mantri for his valuable support and motivation throughout this project work.

We also extend our gratitude to Dr. Uğur Guven for his expertise and help in the field of CFD analysis and his valuable time and efforts towards the completion of this project.

We thank Mr. Ramesh Tandon for his immense help in the field of aero-modeling for fabrication of the wind tunnel model.

ABSTRACT

Bird, bat, and insect flight have fascinated humans for many centuries. Since the late 1990s, the so-called micro air vehicles (MAVs) have attracted substantial and growing interest in the engineering and science communities. Micro Air Vehicles are currently designated with a largest linear dimension of not more than 6-12 inches, which is comparable to the size of small birds or bats, and a flight speed of 10–20 m/s. Equipped with a video camera or a sensor, these vehicles can perform surveillance and reconnaissance, targeting, and biochemical sensing at remote or otherwise hazardous locations. With the rapid progress made in structural and material technologies, miniaturization of power plants, communication, visualization, and control devices, numerous groups have developed successful MAVs. Overall, alternative MAV concepts, based on fixed wing, rotary wing, and flapping wing have been investigated

The MAVs operate in the low Reynolds number regime (10^4 – 10^5) and in comparison to large, manned flight vehicles, have unfavorable aerodynamic characteristics, such as low lift-to-drag ratio. On the other hand, the MAVs' small geometric dimensions result in favorable scaling characteristics, such as reduced stall speed and better structural survivability.

BW 811 and BW 808 are Blended Wing models that were designed at National Aerospace Laboratories in summer of 2009 for remote controlled and autonomous flight respectively.

Aerodynamics and flight performance of BW 811 have been studied in detail. Response of the model to sharp edged wind gust has been considered. The wind tunnel model for BW 811 has been fabricated and the comparison of software results and wind tunnel results is presented.

CONTENTS

1. Introduction	1
1.1. Objective.....	1
1.2. Literature survey	1
1.3. Applications of Micro Aerial Vehicles	5
2. Weight and Cost Estimation	7
3. Aerodynamic Study and Analysis	8
3.1. Low Reynolds number airfoils	8
3.2. Airfoil Analysis and Selection.....	9
3.3. Winglets	10
3.4. Planform Analysis and Selection.....	12
3.5. Computational Results	14
3.6. Flow Illustrator	16
3.7. BW 811 Features	18
4. Performance and Stability	19
4.1. The Drag Polar.....	19
4.2. Cruise performance	20
4.3. Take-off performance	21
4.4. Aerodynamic centre, centre of gravity and static margin	23
4.5. Longitudinal Stability	25
4.6. Directional Stability	26
4.7. Wind Sensitivity	27
5. Experimental Results	33
5.1. Wind Tunnel Model.....	33
5.2. Results Comparison	35
6. Concluding Remarks	39
7. Scope of Work and Suggestions for Future Studies	40
REFERENCES	41

List of Figures

Figure No.	Figure Name	Page No.
Fig.1.1.	Pigeon wing and airplane wing comparison	1
Fig.1.2.	Lift generation	2
Fig.1.3.	Wing surface deformation	3
Fig.1.4.	Blended Wing Designs	4
Fig.3.1.	MH 45 Airfoil	9
Fig.3.2.	MH 45 polars	9
Fig.3.3.	Flow visualization of the tip vortex	10
Fig.3.4.	C_L vs α curve for BW 811 (with & without winglet)	11
Fig.3.5.	Selected planform polars	12
Fig.3.6.	Polars for BW 811	13
Fig.3.7.	C_p Distribution	14
Fig.3.8.	Streamlines	15
Fig.3.9.	Flow illustration at the tip ($Re = 1000$)	16
Fig.3.10.	Flow illustration at the tip ($Re = 10000$)	16
Fig.3.11.	Flow illustration at the tip ($Re = 260000$)	17
Fig.4.1.	C_M vs. α curve for BW 811	26
Fig.4.2.	Idealized gust profile	27

Fig.4.3.	Response to a sharp-edged gust	31
Fig.5.1.	Wind tunnel test setup	33
Fig.5.2.	BW 811 Wind Tunnel model construction	34
Fig.5.3.	Effect of winglets on aerodynamic performance	36
Fig.5.4.	Comparison of computational and experimental results	37
Fig.5.5.	Brushless motor	38

List of Tables

Table No.	Description	Page No.
Table 2.1.	Weight and Cost Estimation	7
Table 4.1.	Design summary of BW 811	32
Table 5.1.	Experimental data (model without winglets)	35
Table 5.2.	Experimental data (model with winglets)	35

List of Symbols

C_{Di}	Induced drag coefficient
C_{Do}	Parasite drag coefficient
C_D	Total drag coefficient
C_l	2D Lift coefficient
C_L	3D Lift coefficient
AR	Wing aspect ratio
e	Oswald efficiency factor
D	Total drag (N)
ρ	Air density (kg/m^3)
V	True airspeed (m/sec)
L	Total lift (N)
C_{lmax}	Maximum lift coefficient
W	Airframe weight (grams)
α	Angle of attack
Re	Reynolds's No.
M	Mach No.
C_L/C_D	Aerodynamic efficiency
GC_m	Global pitching moment
C_{VT}	Vertical tail volume coefficient
S_V	Area of vertical tail
S_w	Area of wing
B	Span
T_R	Thrust required
P_R	Power required
R/C	Rate of climb
AC	Aerodynamic centre
CG	Centre of gravity
SM	Static margin

Chapter 1

Introduction

1.1. Objective

Design, Analysis and Development of Micro Air Vehicle

1.2. Literature Survey

1.2.1. Biological Flyers

Birds

Flapping flight is more complicated than flight with fixed wings because of the structural movement and the resulting unsteady fluid dynamics. Conventional airplanes with fixed wings are, in comparison, very simple. The forward motion relative to the air causes the wings to produce lift. However, in biological flight the wings not only move forward relative to the air, they also flap up and down, plunge, and sweep. While flapping, birds systematically twist their wings to produce aerodynamic effects in ways that the ailerons on the wings of conventional airplanes operate. Specifically, one wing is twisted downward (pronated), thus reducing the angle of attack (AoA) and corresponding lift, while the other wing is twisted upward (supinated) to increase lift. With different degrees of twisting between wings, a bird is able to roll. The key features that seem desirable are modification of camber and flexing of the wing plan form between upstroke and down stroke, twisting, area expansion and contraction, and transverse bending.

- *Unpowered Flight: Gliding and Soaring*

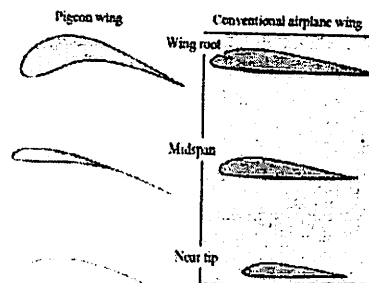


Fig.1.1. Pigeon wing and airplane wing comparison

Flying animals usually flap their wings to generate both lift and thrust. But if they stop flapping and keep their wings stretched out, their wings actively produce only lift, not thrust. Thrust can be produced by gravity force while the animal is descending. When this happens, we call them gliders. In addition to bats and larger birds, gliders can also be found among fish, amphibians, reptiles, and mammals.

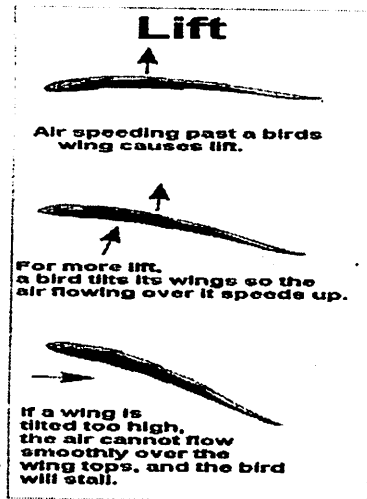


Fig.1.2. Lift generation

To maintain level flight, a flying animal must produce both lift and thrust to balance the gravity force in the vertical direction and drag in the horizontal direction, respectively. Because gliding occurs with no active thrust production, an animal always resorts to the gravity force to overcome the drag. In gliding, the animal tilts its direction of motion slightly downward relative to the air that it moves through. When the animal tilts downward, the resulting angle between the motion direction and the air becomes the gliding angle. The gliding angle directly controls the lift-to-drag ratio. The higher this ratio, the shallower the glide becomes.

While gliding animals take a downward tilt to have the gravity-powered flight, many birds can ascend without flapping their wings, and this is called soaring. Instead of using gravity, soaring uses energy in the atmosphere, such as rising air currents.

- *Powered Flight: Flapping*

An alternative method to gliding used by many biological flyers to produce lift is flapping-wing flight. The similarities between the aerodynamics of a flapping wing and that of a rotorcraft, although limited, can illustrate a few key ideas. Take for example the rotors of a helicopter, which rotate about the central shaft continuously. The relative flow

around the rotors produces lift. Likewise, a flapping wing rotates, swings in an arc around its shoulder joint, and reverses direction every half stroke. Helicopters tilt the rotational plane of rotors from horizontal to forward. The steeper the tilts of the rotor, the faster the helicopters accelerate. Biological flyers also tilt their flapping stroke plane: down and forward on the downstroke, and up and backward on the upstroke. To fly faster, biological flyers make the stroke more vertical by increasing the up-and-down amplitude of the movements.

- *Hovering*

Whether a flying animal can hover or not depends on its size, moment of inertia of the wings, degrees of freedom in the movement of the wings, and the wing shape. As a result of these limitations, hovering is mainly performed by smaller birds and insects. Larger birds can hover only briefly.

Insects

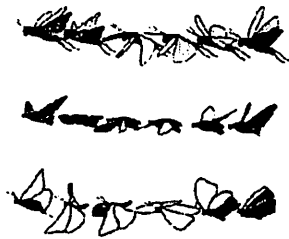


Fig.1.3. Wing surface deformation

Winged insects have evolved complex flight controls and power sources that are the essence of form and function as far as micro flight is concerned. As such, they have played an important role in the development of flight mechanisms and body designs for micro-air vehicles. By all conventional means insects should not be able to fly. To support an insect's body weight, the wings must produce two to three times more lift than has been shown in conventional fixed wing flight studies. Insects accomplish this in two ways. Some insects use a fling mechanism of clapping their wings together on the upstroke and then flinging them apart during the down stroke, causing a vortex around each wing that helps to create lift. However, most insects rely on a leading edge vortex (LEV) that is created by a wing stall during flight. This type of stall creates a very strong span wise flow across the wing causing a LEV to corkscrew to the wing tip producing lift.

1.2.2. Micro Air Vehicles

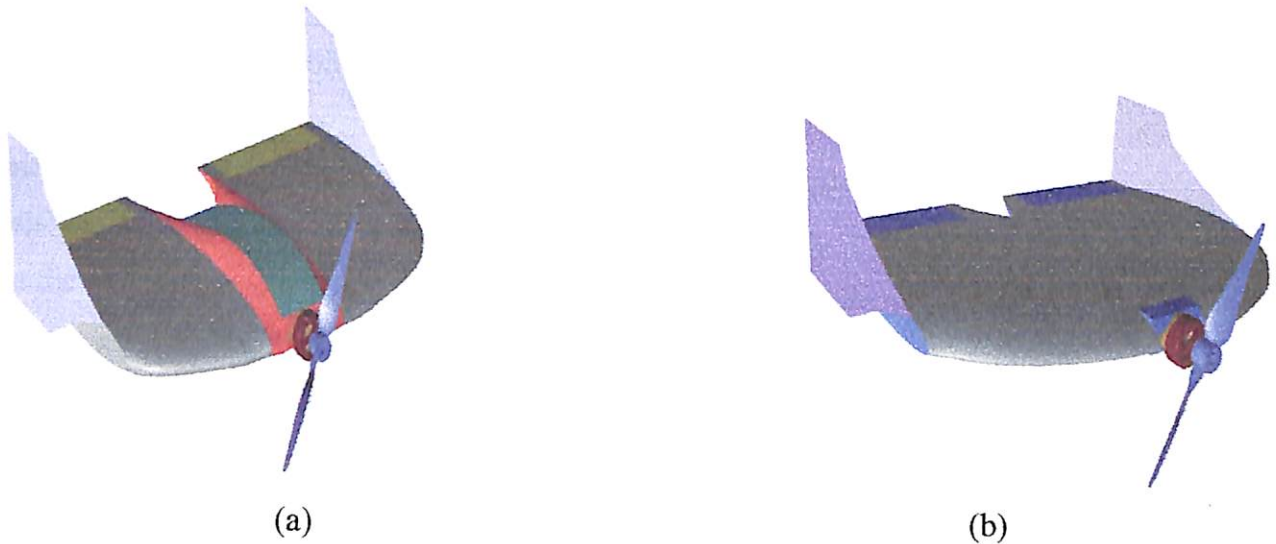


Fig.1.4. Blended wing designs: (a) BW 808 (b) BW 811

These are Blended Wing Micro Air Vehicles that were designed at National Aerospace Laboratories, Bangalore during Summer Internship in June-July 2009.

Literature survey has revealed that tremendous amount of research is being carried out in the area of design and development of MAVs for various goals. Aerodynamic designs of MAVs, reported so far, have employed different kinds of efficient lift generation system viz., fixed wing, flapping wings, flexible wing and rotary wings or their combination [2]. The blended wing design is one of the recent areas of research within fixed wing MAVs because of its improved performance. Research has shown that blending the wing and fuselage and adding winglets provides a reduction in the extent of the wing-tip vortices and refocuses them away from the lifting surface [7, 15].

MAVs are characterized by Aspect Ratio close to unity [3]. For a given lift, a low AR wing has higher drag as compared to a high AR wing. Aspect Ratio also has a direct impact on stall angle. Since the wingtips in a low aspect ratio wing have a lower effective angle of attack, the wing will tend to stall at a higher angle than a high aspect ratio wing. With decrease in Aspect Ratio, the lift curve slope decreases and hence stalling is delayed [11].

The available literature on aerodynamic performance of airfoils at low Reynolds number [6] show poor performance and lower aerodynamic efficiency compared to higher Reynolds number [13]. This is mainly due to the flow separation at relatively low angle of attack. The laminar separation bubbles in this flow regime result in large parasite drag and low C_{Lmax} [8]. The most commonly used low Reynolds number airfoils are Selig, Eppler, Wortmann, Althaus, MH, Drela and Zimmerman [4, 5].

Numerous wind Tunnel experiments have been done on a variety of planform shapes which reveals that for a given maximum dimension and aspect ratio, the inverse Zimmerman planform offers the most efficient shape for MAVs [3].

Research suggests that the addition of winglets to an MAV can improve the lift characteristics and the lift-to-drag ratio of the vehicle significantly. However, one must be careful when choosing a winglet as ill-designed winglet can also reduce the performance of the MAV [7, 14].

1.3. Applications of a Micro Aerial Vehicle

As it is possible to see from the sections above, Microaerial vehicles provide a new frontier in flight mechanics. The applications of Microaerial vehicles have become very diverse as many big aerospace companies as well as organizations are doing extensive work on this subject. There are several applicable uses for Microaerial vehicles that allow for special aerospace applications such as:

- The usage of Microaerial vehicles in military applications. Because of their size and due to their relative stealth caused by the use of composite materials: these type of vehicles can be used for intelligence gathering purposes. In fact, these types of Microaerial vehicles are deployed by NATO in Western countries extensively.
- Microaerial vehicles are also used to provide background data on meteorological situations. Especially in instances of severe weather disturbance, types of microaerial vehicles are deployed in these areas to provide online feedback data. Due to their relatively low cost and their versatility, these vehicles provide an intelligent choice.
- Microaerial vehicles are also used for some simple remote sensing and reconnaissance applications for various survey works. Again due to their versatility, there are several instances in which a microaerial vehicle can be used to provide the necessary data online to the user conducting the geological or geographic survey.

- In a study conducted by the NASA, it has been stated that it is possible to use Microaerial vehicles to create pockets of communications centers in inhospitable conditions. Especially in remote locations where standard non satellite signals are not relayed, it is possible to use these Microaerial vehicles to create simple communications platforms for short periods of time by using a mobile transmission booster strapped on the Microaerial vehicle.

Chapter 2

Weight and Cost Estimation

Equipment	Weight (grams)	Cost (Rs)
Brushless Motor	46	750
Li-Poly Battery (3 pack)	89	1125
Autopilot	39	-
Modem	15	-
Servo (x2)	16	850
Electronic Speed Controller	22	750
Battery Connector	-	90
Propeller (9 in x 5 in)	-	95
Transmitter	-	9900
Receiver	-	1150
Total	300	15000

Table 2.1. Weight and Cost estimation

Chapter 3

Aerodynamic Study and Analysis

The aerodynamics of micro aerial vehicles is greatly affected by the airfoil, operating chord based Reynolds number, planform shape, and wingtip devices like winglets. Airfoils in the low Reynolds number regime show poor performance and low aerodynamic efficiency due to boundary layer separation in laminar flow at a low angle of attack [6, 13]. A number of low Re airfoils were referred and system requirements and preliminary analysis filtered the choices. With low Aspect Ratios (close to unity), the lift curve slope decreases resulting in a delayed stall [11]. For a given lift, a low aspect ratio wing has higher drag as compared to a high aspect ratio wing. Literature survey shows that research has been carried out for a number of planform shapes like rectangular, elliptical, Zimmerman, inverse Zimmerman etc. [3]. For the present application, maximum surface area was desired to minimize C_{Lreq} for a given lift. Winglets with 90° cant angle serve as double symmetric fin for directional stability and also help reduce the induced drag [14].

3.1. Low Reynolds number airfoils

Based on the study of various technical papers on MAV it was found out that because of their small chord length and low velocities, the flight of MAVs has very low Reynolds numbers compared to other manmade flying vehicles. MAVs fly at Reynolds numbers around 10^4 – 10^5 . MAV's flight regime presents many complicated issues that airfoils at higher Reynolds numbers do not experience. Because of the low flight speed and small size of the MAV, airflow over the wing is predominantly laminar [6]. Laminar boundary layers typically separate as soon as the pressure gradient becomes adverse. In general, for Reynolds numbers less than 5×10^4 , the separated flow will not reattach and the airfoil will stall at low to moderate angles of attack. In general, for Reynolds numbers ranging from between 5×10^4 to 3×10^5 , the separated flow forms a laminar separation bubble in which the flow is initially laminar, separates, then transitions to turbulent and reattaches to the airfoil. This separation bubble can greatly affect the airfoil efficiency. Aerodynamic efficiency can drop so low that it becomes a serious limitation to the MAV design [4].

The most commonly used low Reynolds number airfoils are Selig, Eppler, Wortmann, Althaus, MH, Drela and Zimmerman [5, 23].

3.2. Airfoil Analysis and Selection

A number of airfoils were referred from various technical papers and UIUC (University of Illinois at Urbana-Champaign) database. The detailed XFLR analysis and comparison of the different airfoils can be referred from [1].

The remote controlled model BW 811 requires root thickness of 25mm so the airfoil selected is MH 45 (Fig.4.3). This airfoil has a reflex at the trailing edge, very less camber, hence greater stability.

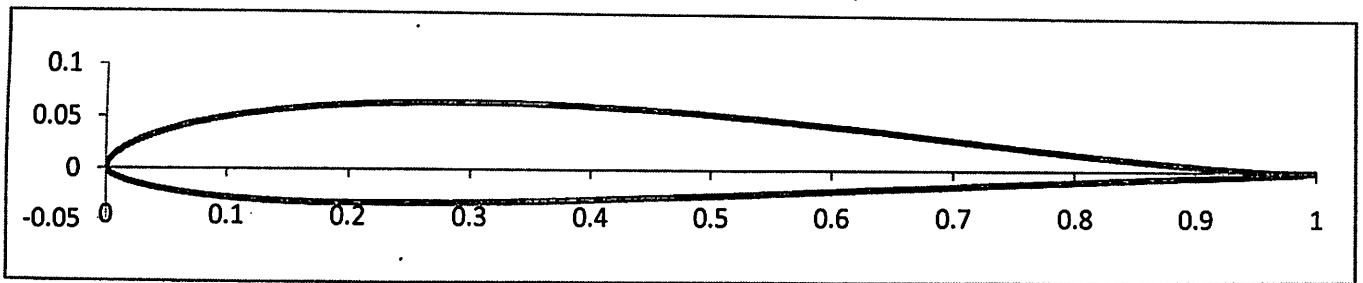


Fig.3.1. MH 45 Airfoil

The polars of MH 45 are as follows:

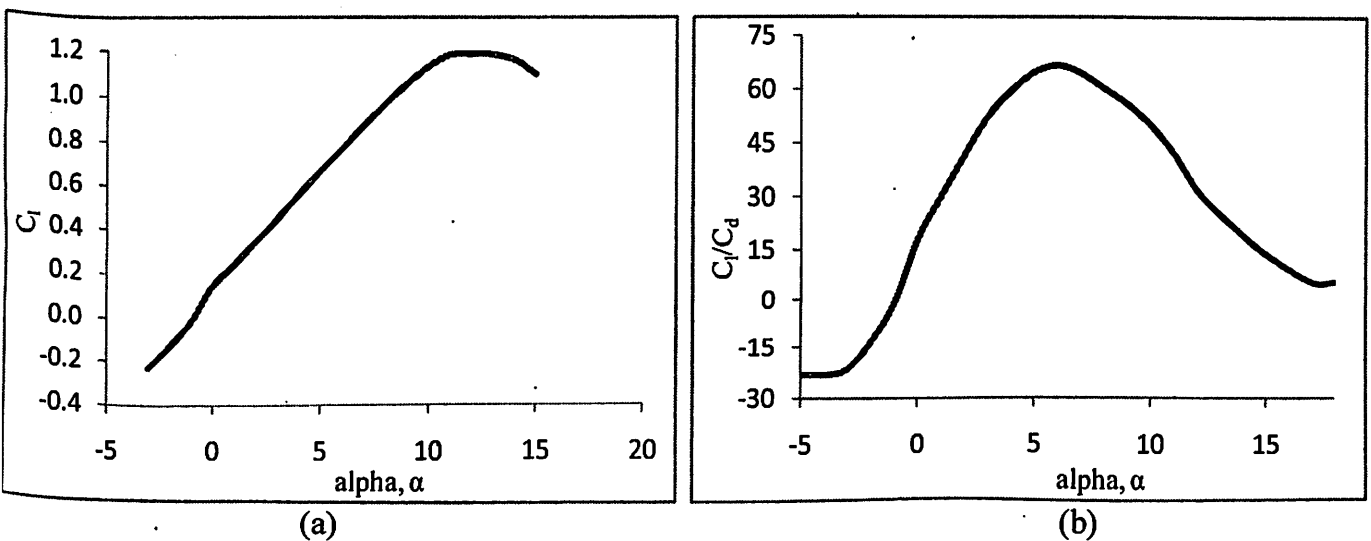


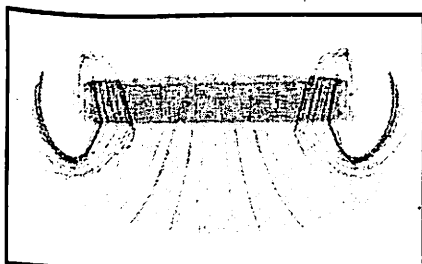
Fig.3.2. MH 45 polars : (a) C_l vs α (b) C_l/C_d vs α

3.3. Winglets

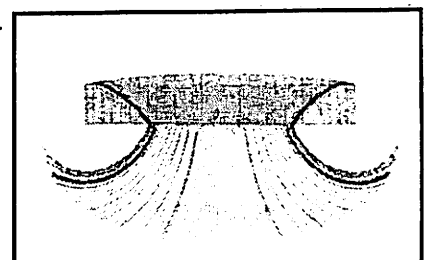
MAV aerodynamics is strongly affected by the wing tip vortices which extend over a significant amount of span. At the tips of any wing, the high pressure flow on the bottom surface of the wing and the low pressure on the top surface of the wing must be equal. These are generally not equal along the wingspan as this would lead to non-lifting wing. The existing pressure difference causes the flow from the bottom side to curl to the top creating a tip vortex and downwash at the wing tip. This downwash lowers the effective lift and leads to an increase in drag. This additional drag is called induced drag or the drag due to lift. The drag increase is due to the tip vortex that causes energy loss in the flow. Induced drag depends only on the lift and the span of the wing and increases rapidly as the wingspan decreases. So increase in span would reduce induced drag but in the present case, due to dimensional constraints, addition of winglets is one of the most feasible options for reduction in induced drag.

$$D_i = \frac{C_L^2}{\pi A} \frac{\rho V^2}{2} \quad C_{Di} = \frac{C_L^2}{\pi A} \left(\frac{C_L}{C_D} \right)$$

The motivation for the use of winglets is to prevent or restrict the imminent downwash at the wingtips. Winglets can increase the performance by decreasing the induced drag. Although the addition of winglets does increase the surface area of the vehicle thus leading to higher frictional drag. It has also been observed that increasing the wingspan does lead to similar reduction in induced drag as addition of a winglet does. Addition of winglet moves the tip vortex up and away from the main wing (Fig.3.3). Thus causing less downwash at the wing and resulting in an increase in lift obtained with the wing. [7, 14, 16]



(a)



(b)

Fig.3.3. Flow visualization of the tip vortex: a) with winglet b) without winglet

Blending the wing and fuselage and adding winglets provides a reduction in the extent of the wing-tip vortices and refocuses them away from the lifting surface [7, 15]. A low aspect ratio wing at low Re features a tip vortex that can extend a distance up to 60% of the chord in the span wise direction. This large tip vortex is a source of drag and decreased lift. When winglet is added to the wing the size of tip vortex is decreased and moved off the lifting surface. Flow visualization & wind tunnel results show that adding winglets make a noticeable difference in $C_{L,\alpha=0}$, $C_{L,max}$ and C_D for a given C_L , but adding winglet increases the overall dimensions of MAV unless the winglets are attached at a 90° cant angle. A noticeable change in the lift and drag were not seen until the cant angle of the winglet was varied from 90° position. As the cant angle was decreased towards the horizontal, an expected increase in the lift was observed. This is due to the larger projected area of winglet onto the plane of the wing.

Fig.3.4 compares the performance of BW 811 with and without winglets [1].

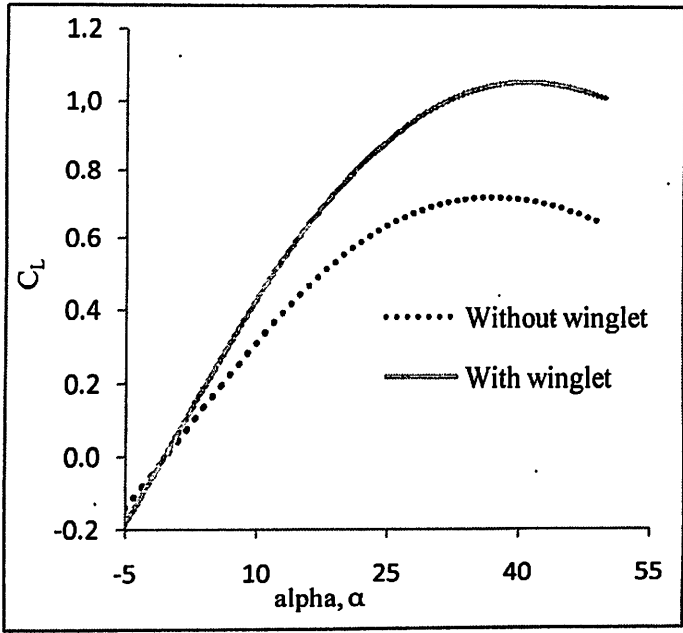


Fig.3.4. C_L vs. α curve for BW811

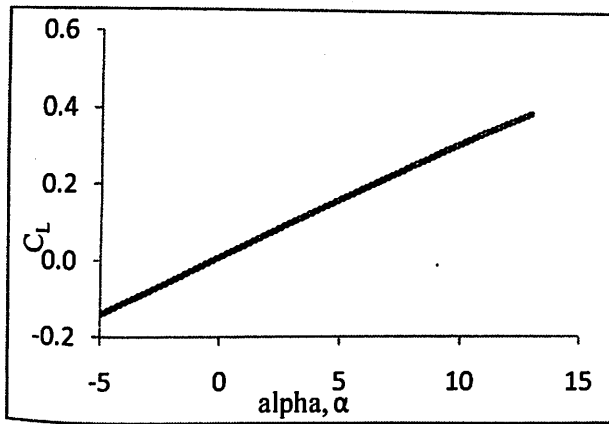
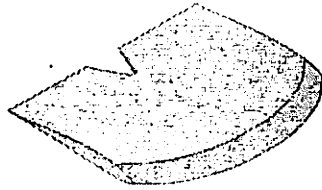
With the addition of winglets, there is a significant increase in lift and aerodynamic efficiency of the MAV.

3.4. Planform Analysis and Selection

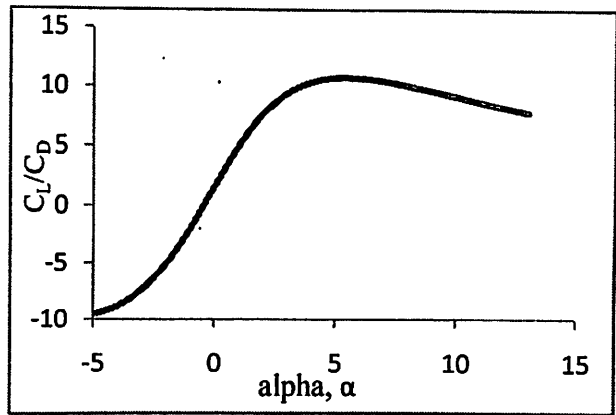
The initial planform shapes were modeled in CATIA and analyzed using XFLR5. Initially the planforms were analyzed without winglets and after selection of the final planform, the analysis was done with winglets.

The results may be referred from [1].

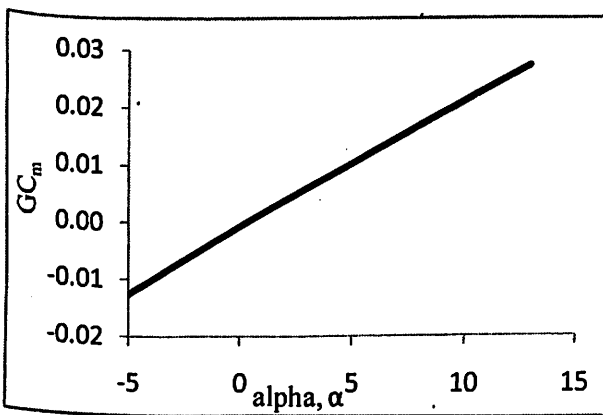
The polars of the selected planform shape are as follows.



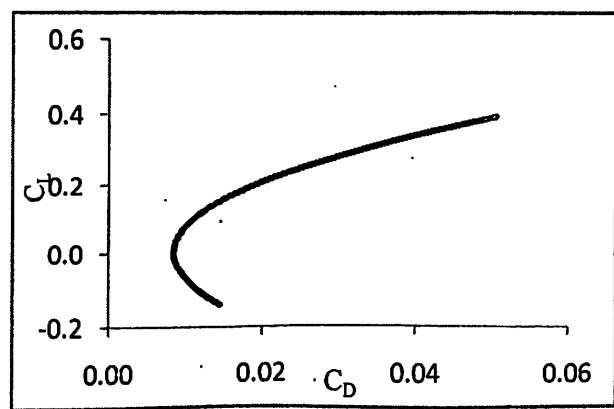
(a)



(b)



(c)

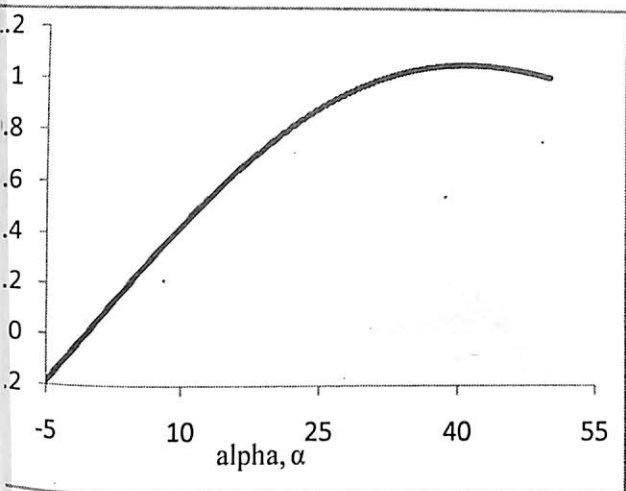
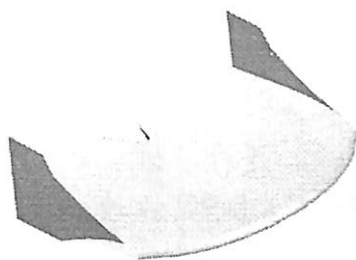


(d)

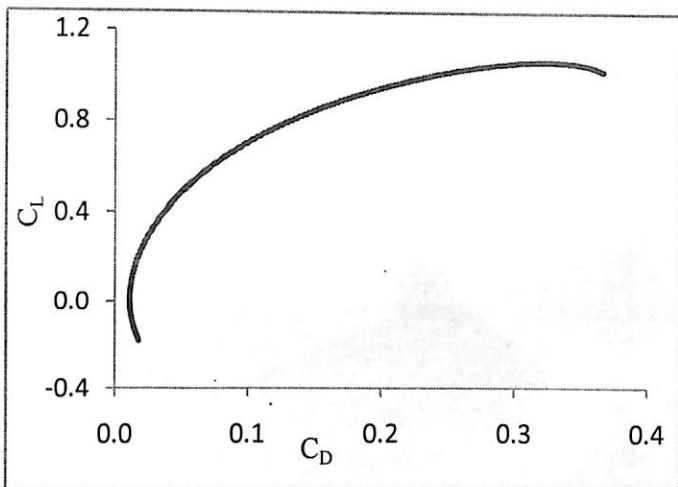
Fig.3.5. Selected planform polars: (a) C_L vs α (b) C_L/C_D vs α (c) C_m vs α (d) C_L vs C_D

From the polars and the winglet study explained above, two models were selected, BW 808 for autopilot accommodation and BW 811 to be remotely controlled.

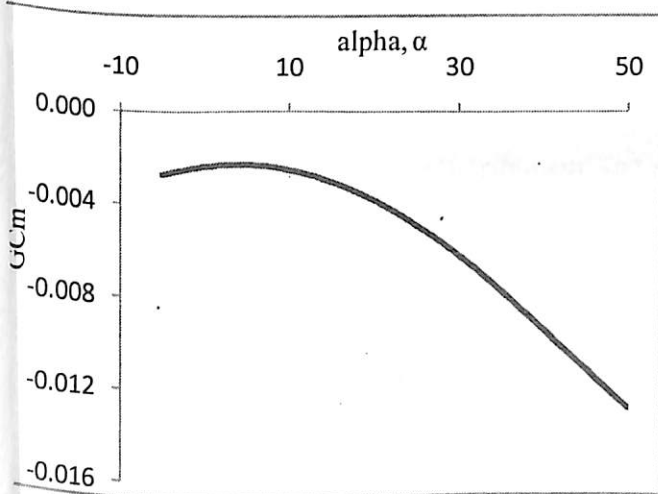
The XFLR5 polars for BW 811 are given below.



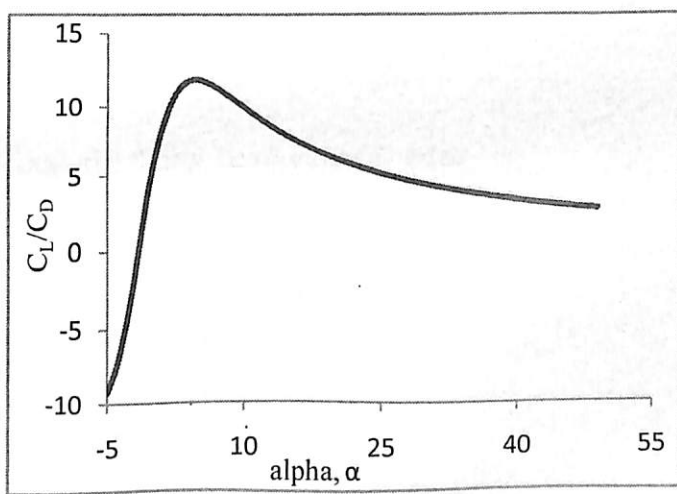
(a)



(b)



(c)



(d)

Fig.3.6. Polars for BW 811:(a) C_L vs α (b) C_L/C_D vs α (c) C_m vs α (d) C_L vs C_D

3.5. Computational Results

3.5.1. C_p Distribution

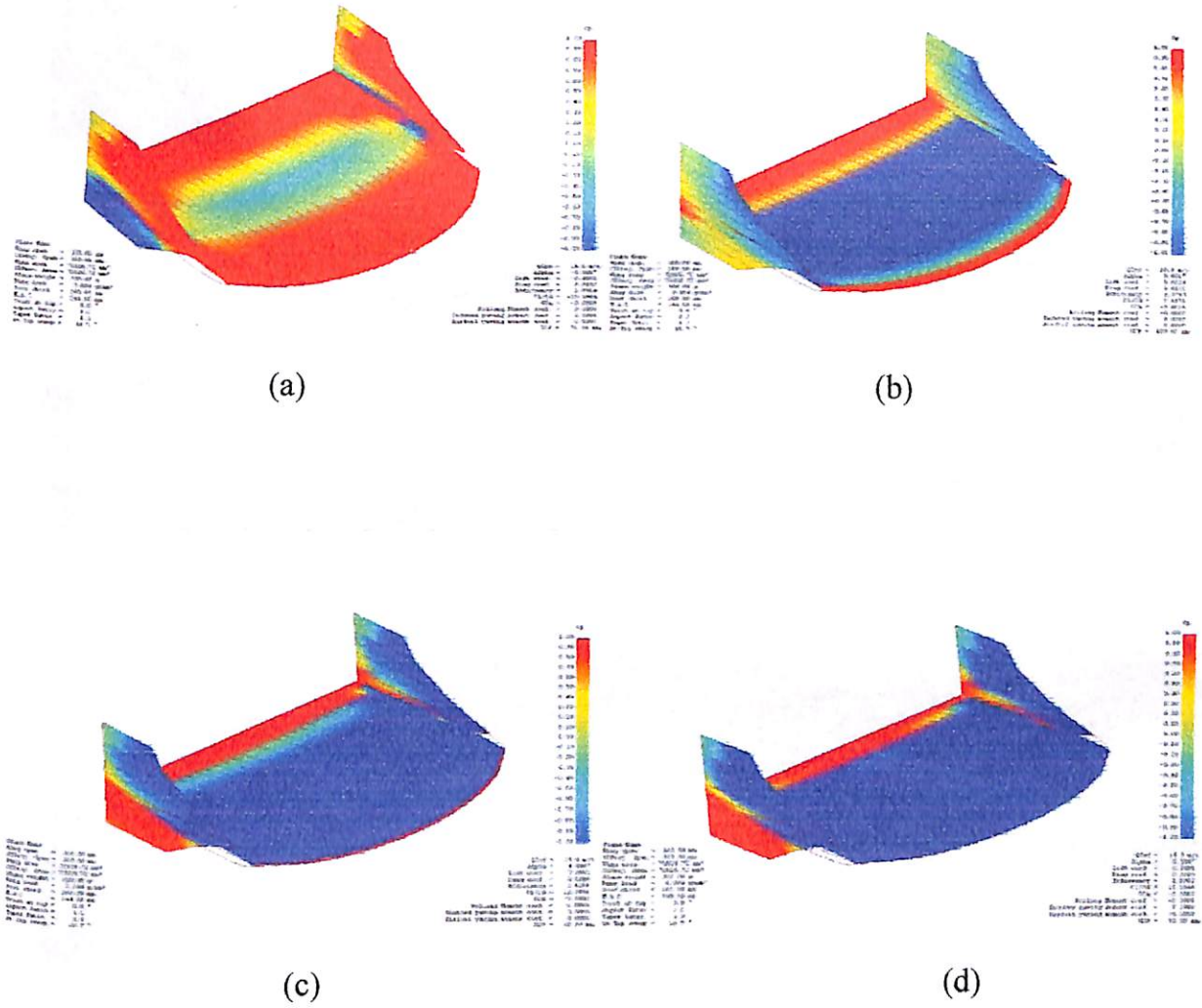
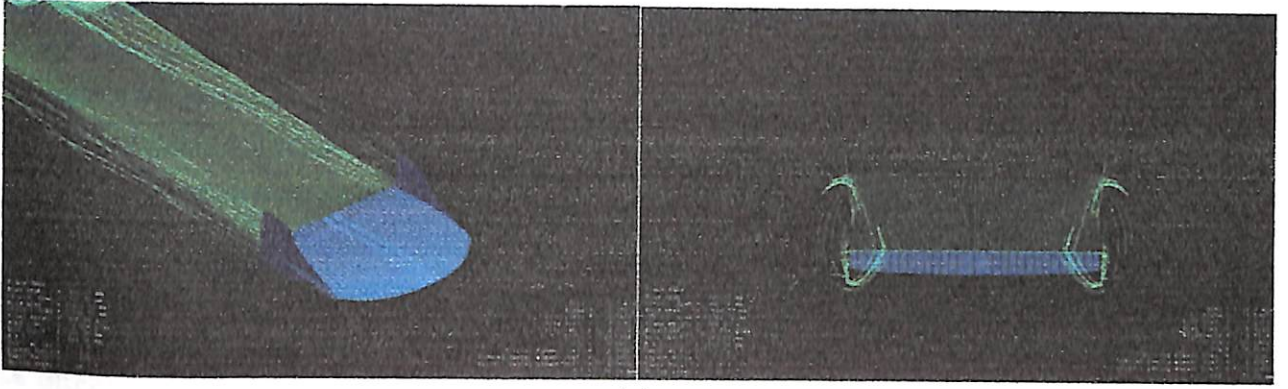
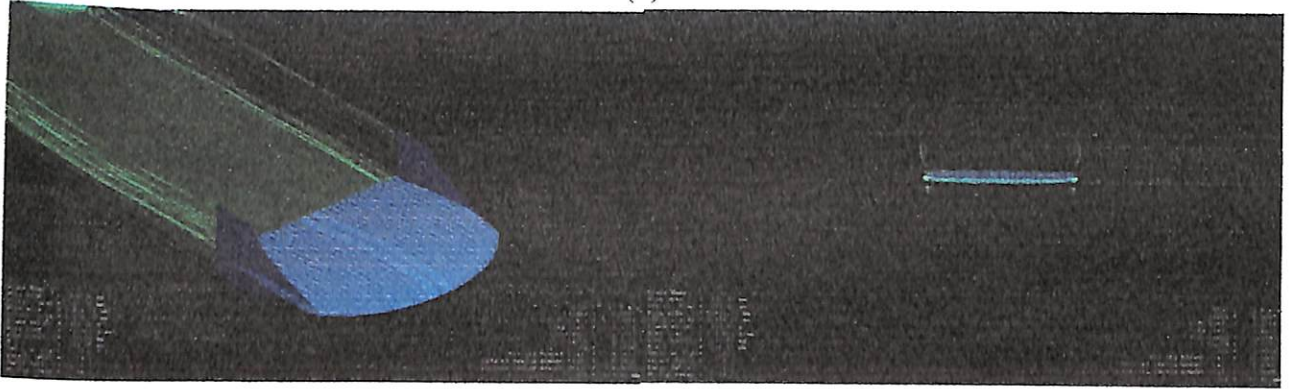


Fig.3.7. C_p Distribution: (a) -5 deg (b) 0 deg (c) 4 deg (d) 8deg

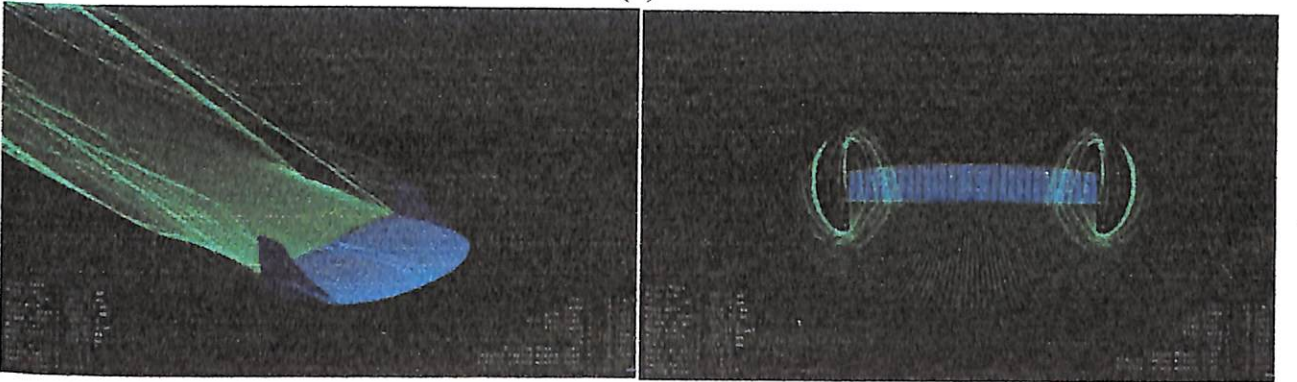
3.5.2. Streamlines



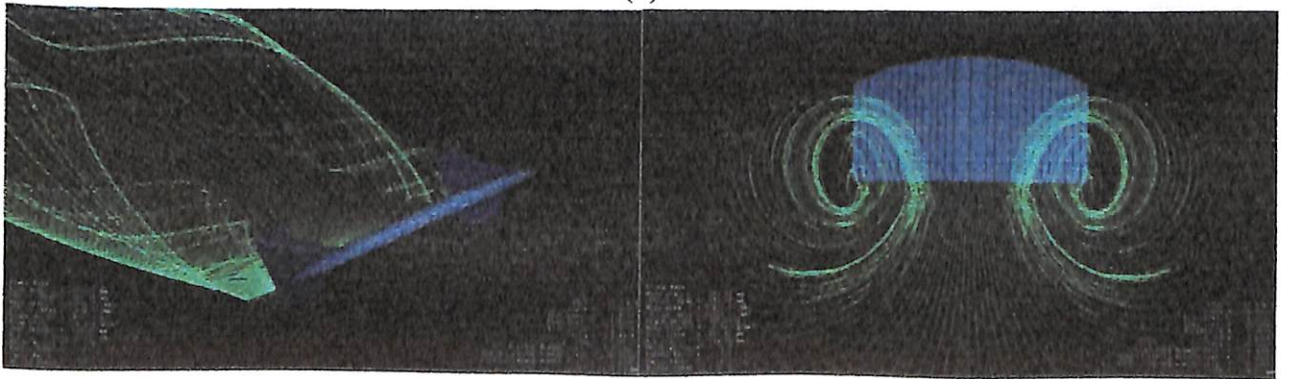
(a)



(b)



(c)



(d)

Fig.3.8.Streamlines: (a) -5 deg (b) 0 deg (c) 8deg (d) 39 deg (stall)

3.6. Flow Illustrator

Easy to use, Flow Illustrator [29] is a webpage program that enables the visitor to make his/her own movies of fluid flows for educational purposes, presentations and recreation. The Movie Maker allows one to upload a picture of their own design and create a movie of the flow past this body. The movie duration, speed, and other parameters can also be specified. This level of flexibility and efficiency is made possible by an original fast algorithm for flow calculations, specially designed for this purpose.

The different views of the BW 811 model were uploaded on the Flow Illustrator webpage and the results are as follows:

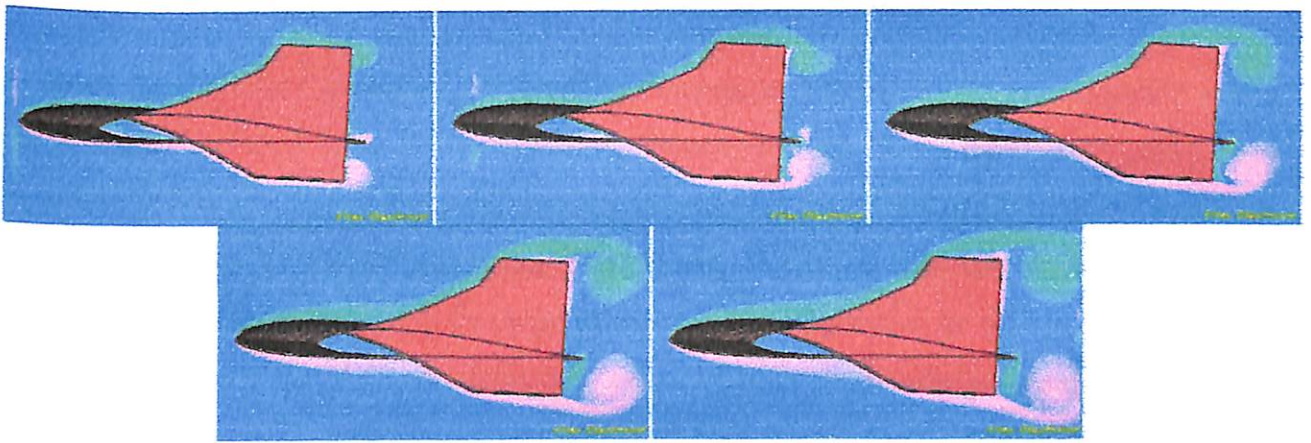


Fig.3.9. Flow illustration at the tip ($Re = 1000$)

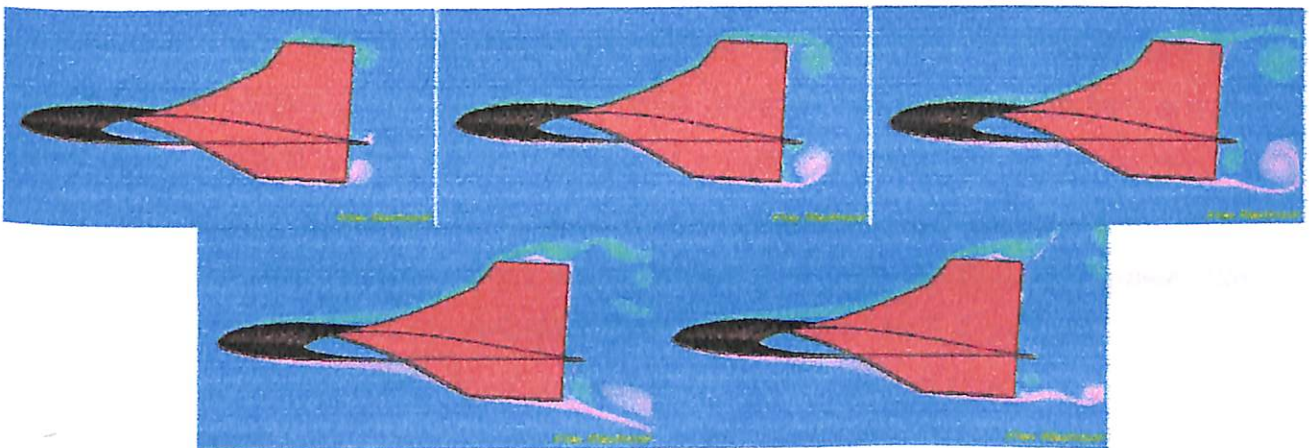


Fig.3.10. Flow illustration at the tip ($Re = 10000$)

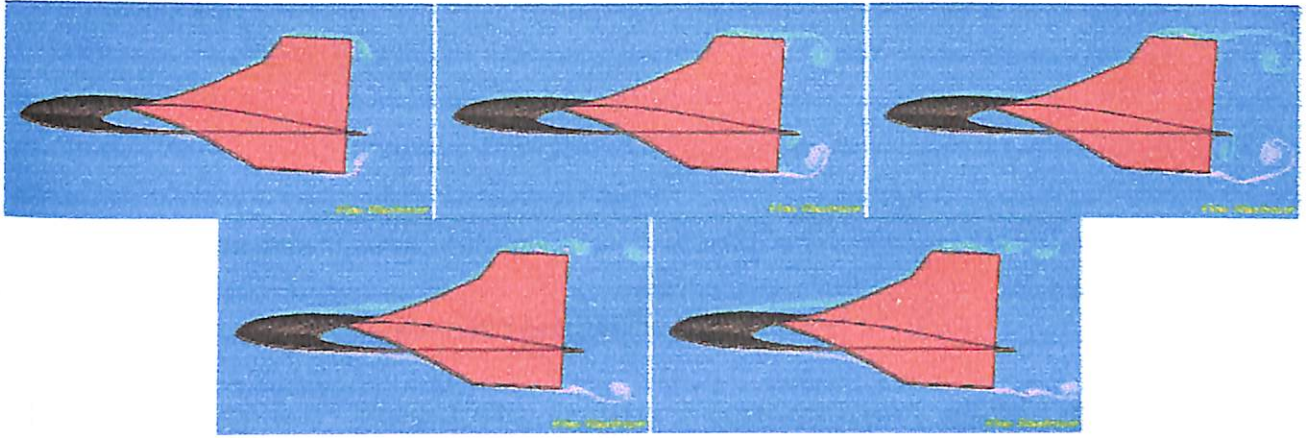


Fig.3.11. Flow illustration at the tip ($Re = 260000$)

The phenomena of flow separation, as illustrated above, is associated with the presence of the boundary layer that wets the entire surface of the vehicle in flight. When the flow separates from the surface, it dramatically changes the pressure distribution over the surface resulting in a large increase in drag, called the pressure drag. The primary flow over the body no longer sees the complete body shape; it sees the body shape upstream of the separation point, but downstream of the separation point it sees a greatly deformed “effective body” due to the large separated region.

The occurrence of separated flow over an aerodynamic body not only increases the drag but also results in a substantial loss of lift. Such separated flow is the cause of airfoil stall.

If the path lines of various fluid elements are smooth and regular, the flow is called laminar flow. In contrast, if the motion of a fluid element is very irregular and tortuous, the flow is called turbulent flow. Because of the agitated motion in a turbulent flow, the higher-energy fluid elements from the outer regions of the flow are pumped close to the surface. Hence, the average flow velocity near a solid surface is larger for a turbulent flow in comparison with laminar flow. Immediately above the surface, the turbulent flow velocities are much larger than the laminar flow values. Due to this frictional effects are more severe for a turbulent flow. But turbulent flow has a major redeeming value; because the energy of the fluid elements close to the surface is larger in a turbulent flow, a turbulent flow does not separate from the surface as readily as laminar flow. If the flow over a body is turbulent, it is less likely to separate from the body surface, and if flow separation does occur, the separated region will be smaller. As a result the pressure drag due to flow separation will be smaller for turbulent flow.

From the above figures it may be observed that at higher Reynolds No. flow does not separate as readily as it does for the lower Reynolds No. cases.

3.7. BW 811 Features

The various features of the planform are listed below-

1. The planform is of blended wing type i.e. it does not have a fuselage for housing the payload and other components.
2. The plane is impact resistant i.e. the airframe is reusable
3. The body is streamlined.
4. In the blended wing design there is no fuselage-wing junction so there is minimal interference drag.
5. Ease of assembly.
6. Reduced downwash and gust control due to winglets/fin.
7. The planform is made up of a single volumetric airfoil.
8. Span-wise transition is negligible.
9. Boundary layer separation is delayed.

Chapter 4

Performance and Stability

An aircraft in flight is subjected to the “four basic forces of flight” – lift, drag, thrust and weight. The aircraft’s response to these four forces determines its performance which includes its velocity, range, endurance, power requirement etc. [10]

MAVs are characterized by a low Aspect ratio and low Reynolds number flow regime [3]. These factors lead to significant deterioration in performance in terms of poor lift-to-drag ratio and high gust sensitivity.

4.1. The Drag Polar

The drag polar [11] for the MAV is given as:

$$C_D = C_{D_0} + C_{D_i} \quad (4.1)$$

Where, C_D = Total drag coefficient

C_{D_0} = Parasite drag coefficient (consisting of profile drag of the wing and fin)

C_{D_i} = Induced drag (lift dependent drag)

$$C_{D_i} = \frac{C_L^2}{\pi e AR} \quad (4.2)$$

Where, C_L = Total lift coefficient

AR = Aspect ratio

e = Oswald efficiency factor

e = 1 (for elliptic planforms)

e < 1 (for all other planforms)

For drag polar of BW 808 and BW 811, refer [1]

4.2. Cruise Performance

$$V_{cruise} = 15 \text{ m/s}$$

For straight and level flight,

$$L=W \text{ and } T=D$$

$$\Rightarrow C_{L,req} = \frac{2W}{\rho V^2 S} = \frac{6}{1.07 \times 15^2 \times 0.0728} \quad (4.3)$$

$$C_{L,req} = 0.3423$$

$$\therefore \alpha_{cruise} = 8^\circ \quad (\text{From XFLR5 results})$$

Drag calculations-

$$C_D = C_{D_o} + C_{D_i}$$

$$C_{D_o} = 0.015 \quad (\text{From literature survey, [20]})$$

$$C_{D_i} = \frac{C_L^2}{\pi e AR_{effective}} \quad (4.4)$$

Where, Oswald efficiency factor (e) = 0.96 (From literature survey, [21])

$$\text{and } AR_{effective} = 1.63$$

$$C_{D_i} = \frac{0.3423^2}{3.14 \times 0.96 \times 1.63} = 0.02384$$

$$C_D = 0.015 + 0.02384$$

$$\Rightarrow C_D = 0.0388$$

Total drag,

$$D = 0.34N$$

Aerodynamic efficiency (lift-to-drag ratio) = 8.81

Thrust required,

$$T_R = \frac{W}{L/D} \quad (4.5)$$

$$\Rightarrow T_R = \frac{3}{8.81} N$$

$$\Rightarrow T_{R,cruise} = 0.3404N \sim 34 \text{grams}$$

Power required,

$$P_R = T_R \times V_{cruise} = 0.3404N \times 15m/s$$

$$\Rightarrow P_{R,cruise} = 5.106W \quad (4.6)$$

4.3. Take-off Performance

$$V_{take-off} = 1.2 V_{stall} \quad (4.7)$$

$$V_{stall} = \left(\frac{2W}{\rho S C_{L,max}} \right)^{1/2} = 8.53 \text{ m/s} \quad (4.8)$$

$$\Rightarrow V_{take-off} = 10.23m/s$$

$$C_{L,req} = \frac{2W}{\rho V^2 S} = \frac{6}{1.07 \times 10.23^2 \times 0.0728}$$

$$C_{L,req} = 0.7360$$

$$\therefore \alpha_{take-off} = 20^\circ \quad (\text{From XFRLR5 results})$$

Drag calculations-

$$C_D = C_{D_0} + C_{D_i}$$

$$C_{D_0} = 0.015$$

$$C_{D_i} = \frac{C_L^2}{\pi e AR_{\text{effective}}}$$

Where, Oswald efficiency factor (e) = 0.96

$$\text{and } AR_{\text{effective}} = 1.63$$

$$C_{D_i} = \frac{0.7360^2}{3.14 \times 0.96 \times 1.63} = 0.1102$$

$$C_D = 0.015 + 0.1102$$

$$\Rightarrow C_D = 0.1252$$

Total drag,

$$D = 0.5103N$$

Aerodynamic efficiency (lift-to-drag ratio) = 5.87

Thrust required,

$$T_{R, \text{take-off}} = 4 \times T_{R, \text{cruise}} \tag{4.9}$$

$$\Rightarrow T_{R, \text{take-off}} = 1.3616N \sim 136 \text{grams}$$

Power required,

$$P_R = T_R \times V_{\text{take-off}} = 1.3616N \times 10.23m/s$$

$$\Rightarrow P_{R, \text{take-off}} = 13.92W$$

Angle of Climb,

$$\sin \theta = \frac{T_{\text{take-off}} - D}{W} = \frac{1.3616 - 0.5103}{3} = 0.2837 \quad (4.10)$$

$$\theta = 16.48^\circ$$

Rate of Climb,

$$R/C = V_{\text{take-off}} \times \sin \theta = 10.23 \text{ m/s} \times 0.2837 \quad (4.11)$$

$$\Rightarrow R/C = 2.902 \text{ m/s}$$

4.4. Aerodynamic Centre, Centre of Gravity and Static Margin

Aerodynamic centre

The concept of the aerodynamic center (AC) is important in aerodynamics. It is fundamental in the science of stability of aircraft in flight. [1, 11]

Aerodynamic Centre is the point along the chord where the pitching moment is independent of angle of attack.

$$\frac{dC_m}{dC_L} = 0 \quad \text{Where } C_L \text{ is the aircraft lift coefficient.} \quad (4.12)$$

For symmetric airfoils in subsonic flight the aerodynamic center is located approximately 25% of the chord from the leading edge of the airfoil. This point is described as the quarter-chord point.

This result also holds true for 'thin-airfoils'. For non-symmetric (cambered) airfoils the quarter-chord is only an approximation for the aerodynamic center.

Centre of gravity

It is the point where all the weight is considered to be acting. The longitudinal static stability of an aircraft is significantly influenced by the position of the center of gravity of the aircraft. The

limitations specified for an aircraft type and model include limitations on the most forward position, and the most aft position, permitted for the center of gravity. [1, 11]

Static Margin

Static margin is a concept used to characterize the static stability and controllability of an aircraft. Static margin is defined as the distance between the aerodynamic centre and centre of gravity of wing. [11, 12]

The response of an aircraft to an angular disturbance such as a pitch disturbance is determined by its static margin. [27]

- If the center of gravity (CG) of an aircraft is forward of the Neutral Point (NP), (negative static margin), the vehicle will respond to a disturbance by producing an aerodynamic moment that returns the angle of attack of the vehicle towards the angle that existed prior to the disturbance.
- If the CG of an aircraft is behind the Neutral Point (NP), (positive static margin), the vehicle will respond to a disturbance by producing an aerodynamic moment that continues to drive the angle of attack of the vehicle further away from the starting position.

The purpose of the reduced stability (low static margin) is to make an aircraft more responsive to pilot inputs. An aircraft with a large static margin will be very stable but slow to respond to the pilot inputs. The amount of static margin is an important factor in determining the handling qualities of an aircraft. [27]

From XFLR5 GC_m vs. α graph,

Aerodynamic centre, AC = 79.5 mm from LE

$$SM = \frac{x_{AC} - x_{CG}}{MAC} \quad (4.13)$$

Where, Mean aerodynamic chord (MAC) = 244 mm

Static Margin should ideally be in between 5-10%

For static margin of 5%, $x_{CG} = 67.3mm$

For static margin of 10%, $x_{CG} = 55.1mm$

Allowable range of CG,

$$55.1mm \leq x_{CG} \leq 67.3mm$$

4.5. Longitudinal Stability

Considering the Longitudinal Static Stability for the MAV:

$$\begin{aligned} C_{m_{\alpha_w}} = & C_{L_w} \left(\frac{X_{cg}}{\bar{c}} - \frac{X_{ac}}{\bar{c}} \right) \cos(\alpha_w - i_w) + C_{D_w} \left(\frac{X_{cg}}{\bar{c}} - \frac{X_{ac}}{\bar{c}} \right) \sin(\alpha_w - i_w) \\ & + C_{L_w} \frac{(Z_{cg})}{\bar{c}} \sin(\alpha_w - i_w) - C_{D_w} \frac{(Z_{cg})}{\bar{c}} \cos(\alpha_w - i_w) + C_{m_{ac_w}} \end{aligned} \quad (4.14)$$

For small angle approximation,

$$C_{m_{0_w}} = C_{m_{ac_w}} + C_{L_{0_w}} \left(\frac{X_{cg}}{\bar{c}} - \frac{X_{ac}}{\bar{c}} \right) \quad (4.15)$$

$$C_{m_{\alpha_w}} = C_{L_{\alpha_w}} \left(\frac{X_{cg}}{\bar{c}} - \frac{X_{ac}}{\bar{c}} \right) \quad (4.16)$$

Taking values from XFLR 5 results [1],

$$X_{CG} = 67.3$$

$$X_{AC} = 79.5$$

$$C_{m,AC} = -0.002$$

$$C_{L_{0,w}} = 0.022$$

$$\Rightarrow C_{m_{0,w}} = -0.0031 \text{ (Should be positive)}$$

$$\Rightarrow C_{m_{\alpha,w}} = -0.001 \text{ (Should be negative)}$$

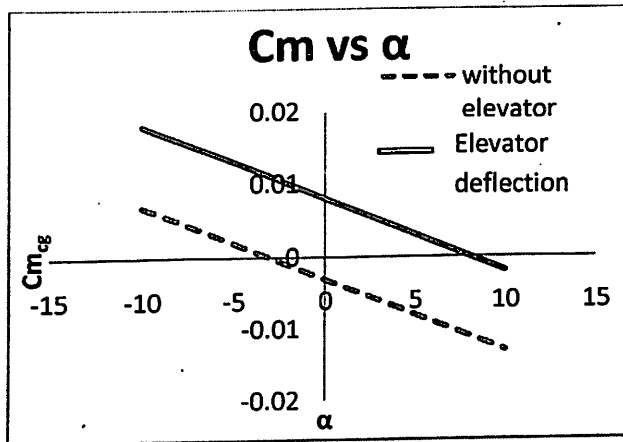


Fig.4.1. C_M vs. α curve for BW 811

To get positive intercept of C_m vs. α curve, elevator deflection is required.

4.6. Directional Stability

Winglet sizing

The vertical tail/winglet sizing was done based on the Vertical tail Volume Coefficient (C_{VT}). The higher this value is, the higher the degree of yaw stability. [18]

$$C_{VT} = \frac{S_v \times L_v}{S_w \times b} \quad (4.17)$$

Where,

Vertical tail volume coefficient (C_{VT}) = 0.04

S_v = Area of vertical tail

Distance between the AC of vertical tail and CG of wing (L_v) = 43.39 mm

Area of wing (S_w) = 72826.72 mm²

Span (b) = 300mm

$$\Rightarrow S_v = 20141.061 \text{ mm}^2$$

4.7. Wind Sensitivity

The first and foremost assumption for this section is that the model is inherently stable and if disturbed by a vertical wind gust, it would eventually return to its original position.

This section aims at studying the response of the model to a sharp edged gust i.e. if the model is disturbed by a sudden vertical wind gust, the amount of time it would take to return to its original position. [27]

Consider the vehicle constrained so that movement is possible only in the vertical direction. This type of motion could be simulated in a wind tunnel. The response of this constrained vehicle subjected to an external disturbance such as wind gust can be examined.

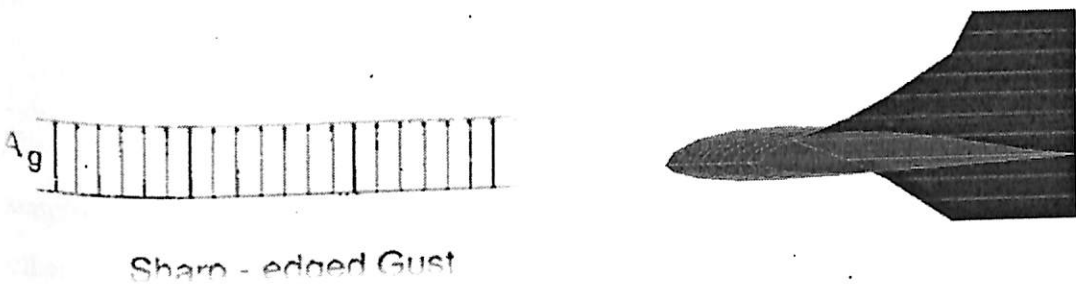


Fig.4.2. Idealized gust profiles

The equation of motion for this example is obtained by applying Newton's second law; that is

$$\sum \text{ Forces in the vertical direction} = m \frac{dw}{dt}$$

$$Z + WT = m \frac{dw}{dt} \tag{4.18}$$

Where Z is the aerodynamic force in the z direction and WT is the weight of the model. If we assume the motion of the MAV will be confined to small perturbations from an initial un-accelerated flight conditions, then the aerodynamic force and vertical velocity can be expressed as the sum of the reference flight conditions plus the perturbation:

$$Z = Z_0 + \Delta Z \quad w = w_0 + \Delta w \tag{4.19}$$

Substituting Eq. (4.19) into Eq. (4.18) yields

$$Z_0 + \Delta Z + WT = m \frac{d}{dt} (w_0 + \Delta w) \tag{4.20}$$

In un-accelerated flight the condition for equilibrium is

$$Z_0 + WT = 0 \quad (4.21)$$

Therefore, Eq. (4.20) reduces to

$$\Delta Z/m = \frac{d}{dt} \Delta w \quad (4.22)$$

The aerodynamic force acting on the model is a function of the angle of attack and time rate of change of the attack and it can be expressed in terms of the stability derivatives as follows:

$$\Delta Z/m = Z_\alpha \Delta \alpha + Z_{\dot{\alpha}} \Delta \dot{\alpha} \quad (4.23)$$

$$\Delta Z/m = C_{z_\alpha} \Delta \alpha QS/m + C_{z_{\dot{\alpha}}} \frac{\Delta \dot{\alpha} c}{2u_0} QS/m \quad (4.24)$$

$$C_{z_\alpha} = -C_{L_\alpha} \quad C_{z_{\dot{\alpha}}} = -C_{L_{\dot{\alpha}}} \quad (4.25)$$

To simplify the analysis the time derivative terms are considered negligible in comparison with the other terms.

The change in angle of attack experienced by the MAV is due to its motion in the vertical direction and also due to the vertical wind gust. The angle of attack can be written as:

$$\Delta \alpha = \frac{\Delta w}{u_0} - \frac{w_g(t)}{u_0} \quad (4.26)$$

Substituting Eq. (4.23) and Eq. (4.26) into Eq. (4.22) and rearranging yields

$$u_0 \frac{d \Delta w}{dt} - Z_\alpha \Delta w = -Z_\alpha w_g(t) \quad (4.27)$$

$$-\frac{u_0}{Z_\alpha} \frac{d \Delta w}{dt} + \Delta w = w_g(t) \quad (4.28)$$

Eq. (4.28) is a first order differential equation with constant coefficients. The system is referred as first order system. Eq. (4.28) can be re-written to have the form:

$$\tau \frac{d \Delta w}{dt} + \Delta w = \left(\tau \frac{d}{dt} + 1 \right) \Delta w = w_g(t) \quad (4.29)$$

$$\tau = -\frac{u_0}{Z_\alpha} \quad (4.30)$$

where

and $w_g(t)$ is the gust velocity as a function of time.

The solution to Eq. (4.29) for a sharp edged or sinusoidal gust can be examined.

The transient response of an airplane to an encounter with a sharp-edged gust can be modeled by expressing the gust profile as a step function:

$$w_g(t) = \begin{cases} 0 & t = 0^- \\ A_g u(t) & t = 0^+ \end{cases} \quad (4.31)$$

where $u(t)$ is a unit step change and A_g is the magnitude of the gust. The solution to Eq. (4.29) for a step input can be obtained by taking the Laplace transformation of the differential equation

$$\tau s \Delta w(s) + \Delta w(s) = w_g(s) \quad (4.32)$$

On solving we get the transfer function of the change in vertical velocity to the vertical gust input.

$$\frac{\Delta w(s)}{w_g(s)} = \frac{1}{\tau s + 1} \quad (4.33)$$

When the forcing function or input is a step change in the gust velocity,

$$w_g(s) = \frac{A_g}{s} \quad (4.34)$$

$$\Delta w(s) = \frac{A_g}{s(\tau s + 1)} \quad (4.35)$$

Expanding Eq. (4.35) by the method of partial fraction and taking the inverse Laplace transformation yields

$$\Delta w(t) = A_g(1 - e^{-t/\tau}) \quad (4.36)$$

The vertical velocity of the MAV grows exponentially from 0 to a final value of A_g .

The parameter τ is referred to as the time constant of the system. The time constant tells us how fast our system approaches a new steady-state condition after being disturbed. If the time constant is small the system will respond very rapidly; if the time constant is large the system will respond very slowly.

The response was developed in form of a MATLAB code taking the following values:

- Time from 0 to 50 seconds
- From XFLR5 results $C_{L,\alpha} = 2.29 \text{ rad}^{-1}$ so using Eq. (4.25) and Eq. (4.30), we get

$$\tau = 6.5502$$

- $A_g = 3.3 \text{ m/s}$ (Gust velocity)
- $u_0 = 15 \text{ m/s}$ (MAV velocity)

So Eq. (4.36) vs. time was plotted in MATLAB using the following code:

```
>> t = 1:50
>> tau = 15/2.29
>> yy = 3.3*(1-exp(-t/tau))
>> plot (t,yy)
```

The following graph was plotted using MATLAB.

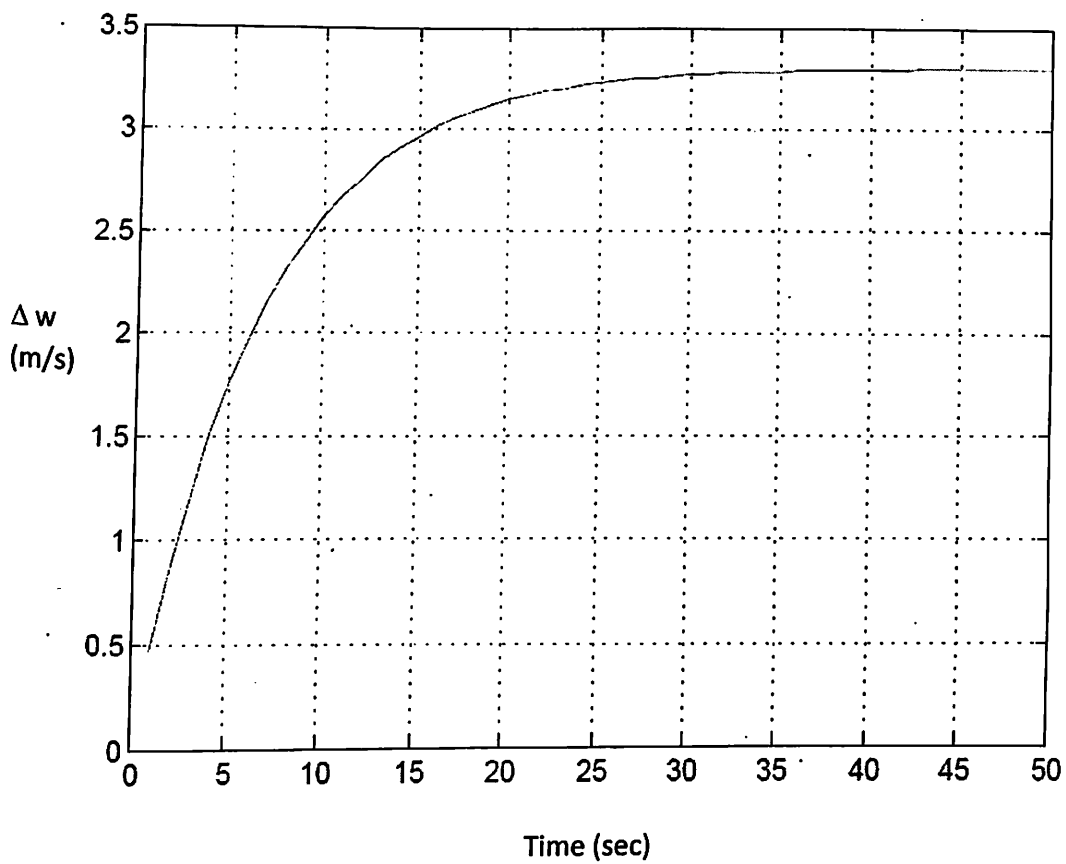
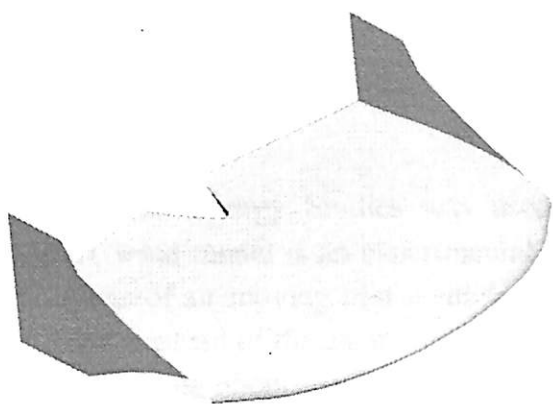


Fig.4.3. Response to a sharp-edged gust

Fig.4.3. shows the response of the MAV to a sharp-edged gust. It is observed that the output of the system approaches the final value asymptotically. It shows that after 25-30 seconds the model will approach a new steady-state condition.

Table 4.1. Design summary of BW 811

AIRFOIL- MH 45				
Airfoil type	Volumetric			
Maximum thickness	9.84% of chord			
Camber	1.71% of chord			
C_{Lmax}	1.187			
$(C_L/C_D)_{max}$	75.98			
α for $(C_L/C_D)_{max}$	6°			
WING		AERODYNAMICS DATA		
Wing type	Blended	C_{Lmax}	1.0581	
Wingspan(b)	300 mm	Aerodynamic Efficiency $(C_L/C_D)_{max}$	11.8597 at $\alpha=6^\circ$	
Area (S)	72826 mm ²	α_{cruise}	8°	
Root chord	260mm	$C_{LCruise}$	0.3423	
Tip chord	200 mm	$(C_L/C_D)_{cruise}$	8.81	
Aspect ratio (AR)	1.24	α_{stall}	39°	
MAC	244 mm	Angle of Climb	16.48°	
Static Margin	5%	Rate of Climb	2.902 m/s	
Aerodynamic centre	79.5 mm from LE	PERFORMANCE PARAMETERS		
Centre of gravity	67.3 mm from LE	V_{cruise}	15 m/s	
VERTICAL FIN (Double Symmetric)		$V_{Take-off}$	10.23 m/s	
		V_{Stall}	8.53 m/s	
Root Chord	180 mm	Thrust Required	Cruise	Take-off
Tip Chord	70 mm		34 grams	136 grams
Height	100 mm	Power Required	Cruise	Take-off
			5.106 W	13.92 W

Chapter 5

Experimental Results

The Subsonic Wind Tunnel at University of Petroleum and Energy Studies was used to determine the aerodynamic data for the BW 811 model. A wind tunnel is an experimental tool used in aerodynamic research. It is used to study the effects of air moving past a solid object. The operation of a wind tunnel is based on the principle that: instead of the air standing still and the aircraft moving at a speed through it, the same effect would be obtained if the aircraft stood still and the air moved at the same speed past it.

Pressure Measurements: Pressure across the surface of the model can be measured if the model includes pressure taps. This can be useful for pressure-dominated phenomenon, but this only accounts for normal forces on the body.

Force Measurements: With strain gauges mounted on the model, one can measure lift and drag created by the model in airflow over a range of angle of attack. It must be noted that there is drag due to the supporting structures along with potential turbulence that will affect the model and introduce errors in the measurements. The supporting structures are therefore typically smoothly shaped to minimize turbulence.



Fig.5.1. Wind tunnel test setup

5.1. Wind Tunnel Model

A Balsa Wood model of BW 811 was fabricated to carry out the wind tunnel test. The fabrication process of the model is explained briefly:

- The different span-wise airfoil sections were exported from CATIA and were cut out on 2 mm balsa sheet.
- Leading and trailing edges were made out of balsa sheets.
- The whole assembly was aligned on the pin board and joined using adhesives.
- The model was removed from the pin board and 1 mm balsa sheet was used for sheeting.
- The mounting rod for wind tunnel testing was attached to the model.
- The winglets were cut out of 2 mm balsa sheets and attached to the model with adhesives.

Fig.5.2. shows the various stages of fabrication of the BW 811 model.

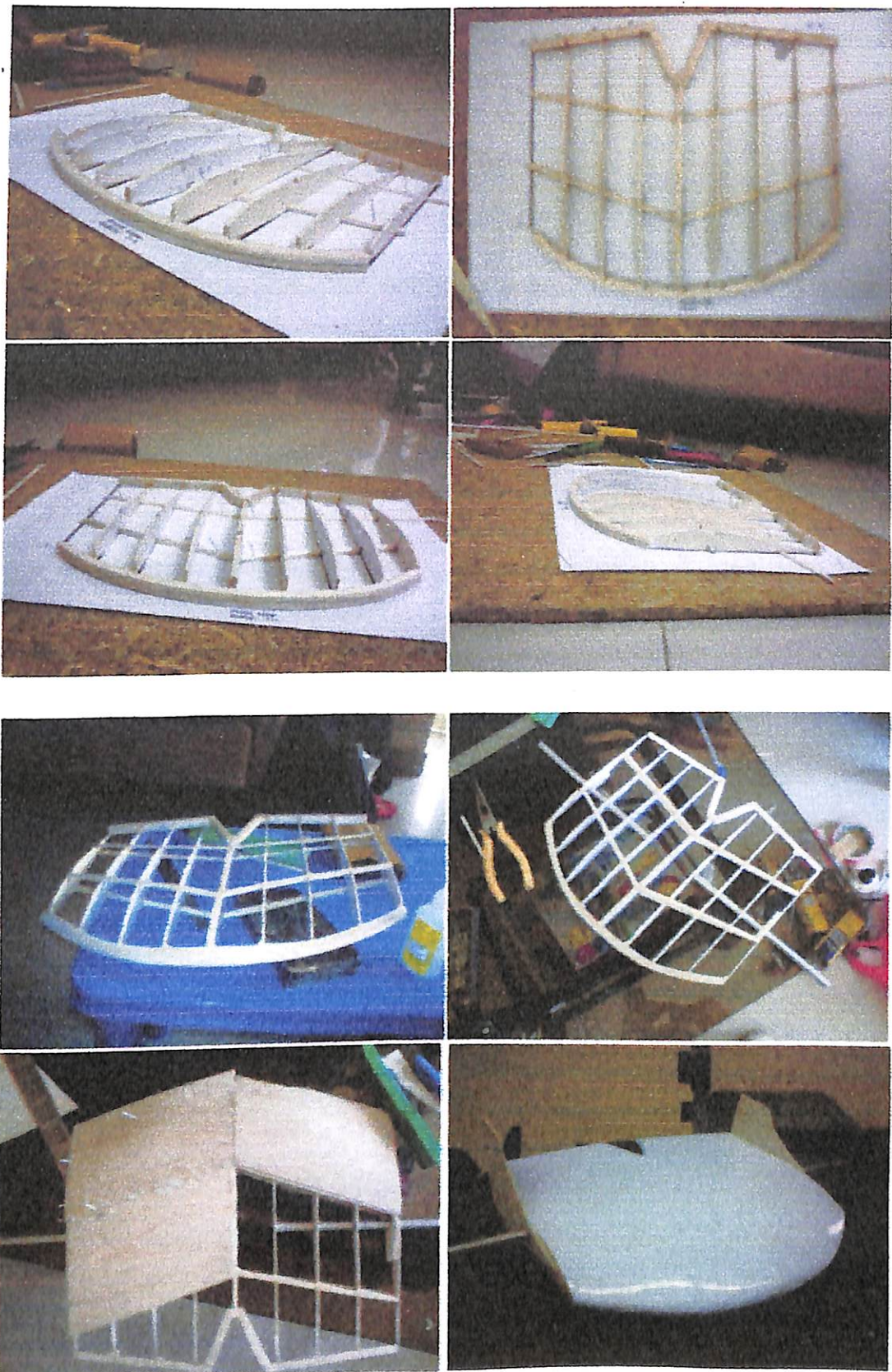


Fig.5.2.BW 811 Wind Tunnel model construction

5.2. Experiments

5.2.1 Experiment No.1

Objective: To study the effect of winglets on the aerodynamic performance of the model.

Procedure: Two wind tunnel were performed, one of the original BW 811 model and the other of the model without winglets.

Results and discussions: Table 5.1 shows the experimental data for both the tests

α	Lift (Kg)	C_L	Drag (Kg)	C_D
0	0.03	0.02898	0.02	0.01932
2	0.06	0.05796	0.02	0.01932
4	0.05	0.0483	0.02	0.01932
8	0.07	0.06762	0.02	0.01932
10	0.25	0.2415	0.04	0.03864
15	0.39	0.37674	0.08	0.07728
20	0.59	0.56994	0.18	0.17388
25	0.71	0.68586	0.35	0.3381
26	0.77	0.74382	0.39	0.37674
27	0.67	0.64722	0.41	0.39606
30	0.47	0.45402	0.43	0.41538

Table 5.1. Without winglets

α	Lift (Kg)	C_L	Drag (Kg)	C_D
0	0.07	0.06762	0.07	0.06762
2	0.09	0.08694	0.07	0.06762
4	0.17	0.16422	0.07	0.06762
8	0.41	0.39606	0.09	0.08694
10	0.46	0.44436	0.1	0.0966
15	0.69	0.66654	0.19	0.18354
20	0.79	0.76314	0.34	0.32844
22	0.84	0.81144	0.38	0.36708
23	0.82	0.79212	0.4	0.3864
24	0.78	0.75348	0.45	0.4347
25	0.64	0.61824	0.45	0.4347
30	0.56	0.54096	0.51	0.49266

Table 5.2. With winglets

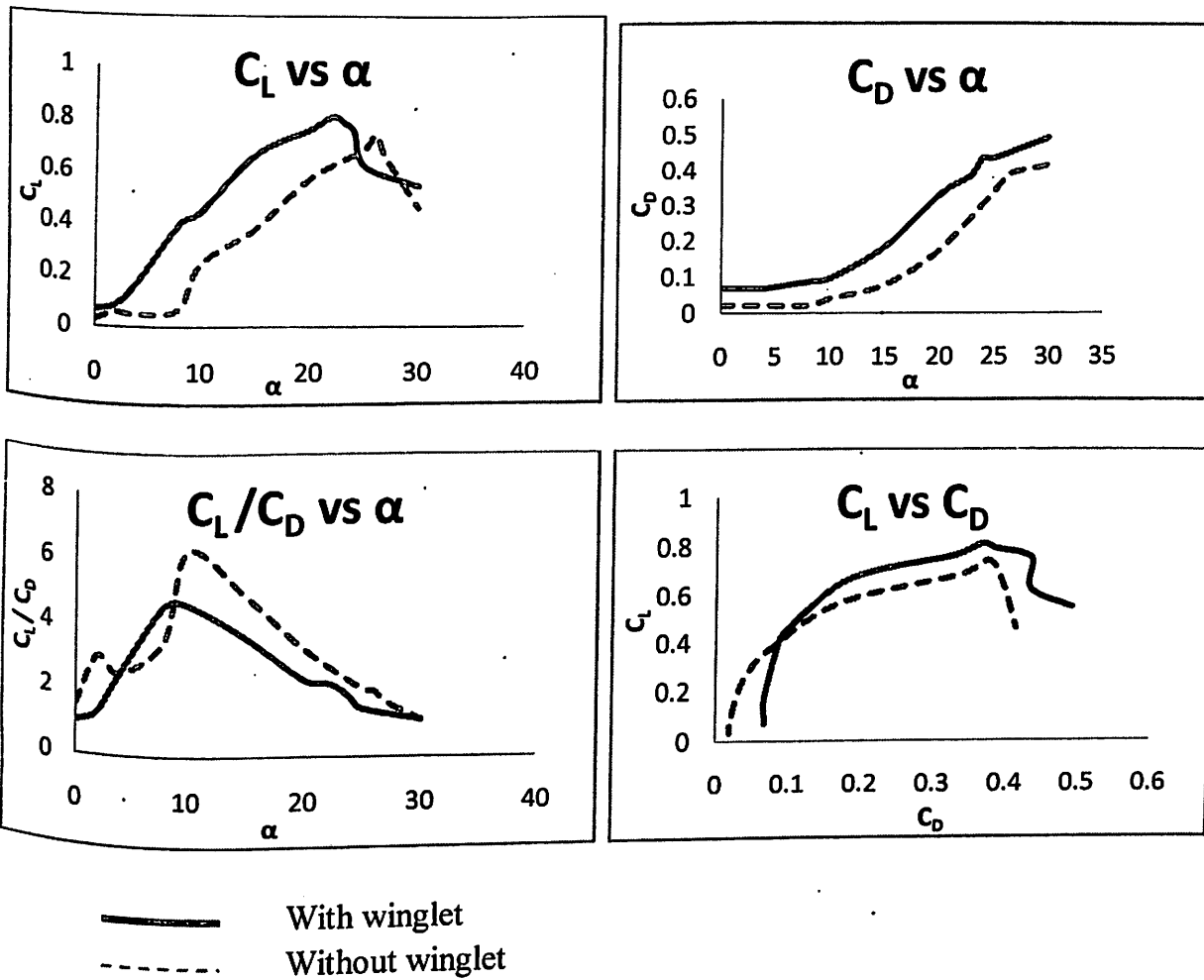


Fig.5.3. Effect of winglets on aerodynamic performance

As already discussed in Chapter 3, winglets serve to increase the lift at the wingtips and reduce the induced drag and downwash but have the penalty of increase in profile drag. From the above data it is observed that use of winglets increases the lift while also increasing the drag.

5.2.2. Experiment No. 2

Objective: To compare XFLR 5 results with wind tunnel results

Procedure: The preliminary analysis of the BW 811 model was done in computational software XFLR5 at National Aerospace Laboratories, Bangalore in June-July 2009. The wind tunnel results were obtained in April 2010 at UPES aerodynamics laboratory.

Results and discussions: Fig.5.3 shows the comparison of wind tunnel and XFLR5 results.

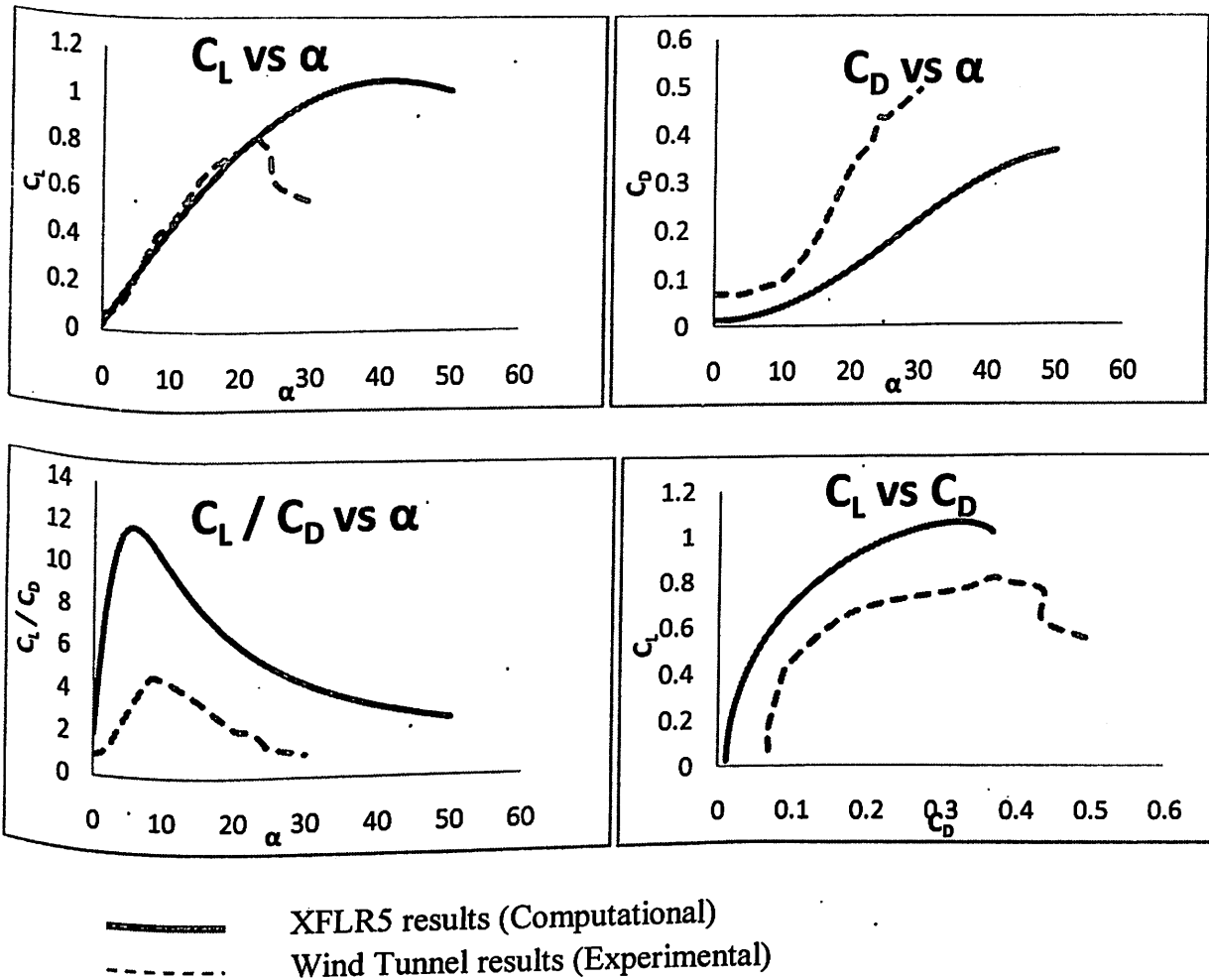


Fig.5.4. Comparison of computational and experimental results

Another wind tunnel test was conducted at $Re = 10^5$ to check the accuracy of results using the standard results for circular cylinder.

Theoretical $C_D = 1.2$

Experimental $C_D = 1.386$

So % age error of wind tunnel = 15.5 %

Power required at cruise:

$$P_r = D \times V$$

$$\Rightarrow P_r = 13.33W$$

So probable power plant required for the flight model:

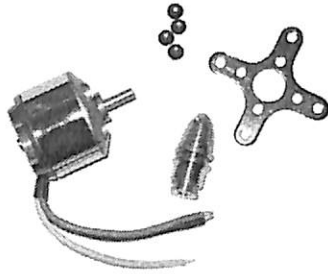


Fig.5.5.Brushless motor

Brushless Motor 2208/14T 150W [28]

Specifications:

1450rpm/Kv

Weight: 46 grams with adapter and mounting plate

Prop: 9x5, 8x4

Approx. power: 125~150

Shaft diameter: 3.2mm

This motor is ideal for models up to 200~500 grams

Chapter 6

Concluding Remarks

- To reduce interference drag and profile drag, blended wing configuration was selected.
- In this study, three main modes of approach were used. Mainly these modes were analytical analysis, experimental analysis as well as computational analysis by using Computational Fluid Dynamics simulation techniques.
- The CFD part was especially emphasized in this study as it allowed for a broader spectrum of analysis regarding the capabilities of this particular Microaerial vehicle.
- The CFD analysis was completed in three different steps. Mainly these were:
 - XFLR5 Software developed and used by MIT Professor Dr. Mark Drela. Various configuration profiles were studied extensively with this method.
 - Flow Simulator designed and developed by Prof. Sergei Chernyshenko, who is currently teaching and researching at the prestigious Imperial College in UK. The vehicle was tested under different Reynolds numbers for performance analysis.
 - GAMBIT was used to model the basic skeletal structure of the Microaerial vehicles. Some simple Post Processing work was done in Fluent to help simulate the behavior of the Microaerial vehicle. However, due to some IT difficulties experiences, the work was cut short; although post Fluent analysis showed great promise in Lifting and Drag Resistance capabilities. Further analysis will be conducted on the Fluent model.
- Wind tunnel test model of BW 811 was fabricated using balsa wood.
- Wind tunnel tests were performed and the acquired experimental data was compared with computational data.
- Performance calculations show that the model is capable of flying.

Chapter 7

Scope of Work and Suggestions for Future Studies

- In future fabrication of a flight model of BW 811 is intended.
- More detailed analysis will be conducted at the junction points of the Microaerial vehicle using detailed FLUENT analysis with a minimum of one million iterations for high level of accuracy. Also further design work is scheduled by using the data obtained from FLUENT to help change the design for better.
- Additional Control surface for gust alleviation.
- Design of altitude-hold autopilot for cruise control.
- Conversion from tractor to pusher configuration.

REFERENCES

1. Abhimanyu Sharma, Govind Singh Dhama, Saniya Chaplod, Smiti Maini, "Design, Analysis and Development of Blended Wing Micro Air Vehicle", NAL Bangalore.
2. Dr. Tom Richardson, "Micro UAVs", February 2007, University of Bristol Seminar.
3. Gabriel Torres and Thomas J. Mueller, "MAV Development: Design, Components, Fabrication and Flight Testing", University of Notre Dame.
4. Carmichael, B.H., "Low Reynolds Number Airfoils Survey", January 1982 NASA Contractor Report 165803.
5. "UIUC Airfoil Coordinates Database," <http://amber.aae.uiuc.edu>
6. Charles O'Neill, "Low Reynolds Number Airfoils", November 2001, MAE 5233
7. Dr. Helen L. Reed and Dr. William S. Saric, "Aerodynamic Studies of Micro Air Vehicles", December 2001, Arizona State University.
8. Dr. Stephen J. Morris and Dr. Michael Holden, "Design of micro aerial vehicles and flight test validation", MLB Company.
9. Anderson, John D., "Fundamentals of Aerodynamics", 2nd Edition, McGraw-Hill, New York, 1991.
10. Anderson, John D., "Aircraft Performance and Design", McGraw-Hill, New York, 1999.
11. Anderson, John D., "Introduction to Flight", McGraw-Hill, New York, 1991.
12. Drela, Mark, XFLR5 v4.16 User Guide, Massachusetts Institute of Technology, Cambridge, Massachusetts, December 2001.
13. Michael I. Kellogg and Dr. W. J. Bowman, "Design of micro aerial vehicles and flight test validation", MLB Company.
14. Dr. Helen L. Reed and Dr. William S. Saric, "On the Effect of Winglets on the Performance of Micro-Aerial-Vehicles", Arizona State University.
15. Prof. Hemendra Arya, "Miniature Aerial Vehicle Airframe Characterization", IIT Bombay.
16. Engineering Sciences Data Unit, "Aerodynamic principles of Winglets", Report No. 98013
17. Nicholas K. Borer, "Design and Analysis of Low Reynolds Number Airfoils", December

2002.

18. http://www.winfoil.com/help/vertical_tail_graph_screen.htm
19. Abdul Huq. A, "Numerical prediction of airfoil aerodynamics at low Reynolds number for MAV application".
20. "Development Of Dart Mav – Fixed Wing Hover-Capable Micro Aerial Vehicle " , Przemyslaw Marek, Warsaw University of Technology
21. "Effect of AR and C_{D_0} on e ", <http://adg.stanford.edu/aa241/drag/induceddrag.html>
22. Morris, S. J., "Design and Flight Test Results for Micro-Sized Fixed-Wing and VTOL Aircraft," 1st International Conference on Emerging Technologies for Micro Air Vehicles, 1997, pp. 117–131.
23. Wei Shyy, "Aerodynamics of Low Reynolds Number Flyers", Cambridge Aerospace Series.
24. "Aerodynamics of Bird and Insect Flight", Wikipedia
25. N. Quin, "Aerodynamic considerations of blended wing body aircraft", University of Sheffield.
26. Sanjay P. Sane, "The Aerodynamics of Insect Flight", University of Washington.
27. R.C. Nelson, "Aircraft Stability and Control"
28. www.indianhobbies.com
29. Flow Illustrator by Prof. Sergei Chernyshenko, <http://chernyshenko.sesnet.soton.ac.uk/>